Stem Cell Reports
Article

ISSCR

OPEN ACCESS

Dynamic Reorganization of Nucleosome Positioning in Somatic Cells after Transfer into Porcine Enucleated Oocytes

Chenyu Tao,[1,5] Juan Li,[1,5] Xia Zhang,[2,3] Baobao Chen,[1] Daming Chi,[1] Yaqiong Zeng,[1] Yingjie Niu,[1] Chengfei Wang,[1] Wei Cheng,[2,3] Wangjun Wu,[1] Zengxiang Pan,[1] Jinmin Lian,[4] Honglin Liu,[1,*] and Yi-Liang Miao[2,3,*]

[1]Department of Animal Genetics, Breeding and Reproduction, College of Animal Science and Technology, Nanjing Agricultural University, Nanjing 210095, PR China
[2]Institute of Stem Cell and Regenerative Biology, College of Animal Science and Veterinary Medicine, Huazhong Agricultural University, Wuhan 430070, China
[3]Key Lab of Agricultural Animal Genetics, Breeding, and Reproduction of Ministry of Education, Huazhong Agricultural University, Wuhan 430070, PR China
[4]Genosys Inc., Shenzhen 518000, China
[5]Co-first author
*Correspondence: liuhonglin@njau.edu.cn (H.L.), miaoyl@mail.hzau.edu.cn (Y.-L.M.)
http://dx.doi.org/10.1016/j.stemcr.2017.06.004

SUMMARY

The nucleosome, the fundamental structural unit of chromatin, is a critical regulator of gene expression. The mechanisms governing changes to nucleosome occupancy and positioning during somatic cell reprogramming remain poorly understood. We established a method for generating genome-wide nucleosome maps of porcine embryonic fibroblasts (PEF), reconstructed 1-cell embryos generated by somatic cell nuclear transfer (SCNT), and fertilized zygotes (FZ) using MNase sequencing with only 1,000 cells. We found that donor PEF chromatin, especially X chromosome, became more open after transfer into porcine oocytes and nucleosome occupancy decreased in promoters but increased in the genic regions. Nucleosome arrangements around transcriptional start sites of genes with different expression levels in somatic cells tended to become transcriptionally silent in SCNT; however, some pluripotency genes adopted transcriptionally active nucleosome arrangements. FZ and SCNT had similar characteristics, unlike PEF. This study reveals the dynamics and importance of nucleosome positioning and chromatin organization early after reprogramming.

INTRODUCTION

The genomes of eukaryotic organisms, from yeast to human, are packaged into nucleosomes, which compact approximately 75%–90% of the whole genome (Field et al., 2008). Nucleosomes consist of approximately 147 bp of DNA wrapped 1.7 times around a histone octamer (Richmond and Davey, 2003; Luger et al., 1997); DNA linkers (20–54 bp) separate the nucleosomes. Nucleosomes are the fundamental structural units of genomes and form the basis for higher-order packaging into chromatin. Nucleosomes cover much of the genomic DNA, except for some specific functional regions, such as promoters and enhancers, which are relatively devoid of nucleosomes (Kaplan et al., 2009). Recent studies show that the canonical nucleosome arrangement (−1, nucleosome depletion region [NDR], +1, +2, etc.) surrounding the transcriptional start site (TSS) is required for gene activation (Segal et al., 2006; Lee et al., 2007).

The current approach for creating genome-wide nucleosome maps is digestion by micrococcal nuclease, which can generate mononucleosomes, followed by sequencing (MNase-seq). The first nucleosome downstream of a TSS exhibits differential positioning in active and silent genes, which indicates how nucleosomes in the TSS region influence gene expression. Many studies have shown that promoter regions are largely devoid of nucleosomes (Bernstein et al., 2004; Lee et al., 2004).

The traditional method of using a micromanipulator to perform somatic cell nuclear transfer (SCNT) is still commonly used; however, the enucleation technique of handmade cloning (HMC), performed using a bisection blade, is being adopted by an increasing number of researchers (Du et al., 2007; Kurome et al., 2008). For HMC two fusion steps, which each contribute half of the cytoplasm, are required to ensure sufficient cytoplasm in the embryo. Thus, SCNT-HMC embryos contain approximately 100%–125% of the original cytoplasmic volume and have good developmental capacity (Du et al., 2007; Kragh et al., 2009; Li et al., 2006, 2015). Following removal of the zona pellucida, oocytes are bisected with a microblade into two halves. Each half oocyte is prepared individually and then fused with a single donor cell and another half oocyte. Both methods are technically difficult and require precious samples, so little work has been performed on nucleosome phasing during the reprogramming of somatic cells into totipotent cells by SCNT (Vajta et al., 2003; Yoshioka et al., 2002).

In our study, we established a method for generating genome-wide maps of nucleosomes using as few as 1,000 cells. First, we made 1,000 SCNT-HMC embryos and

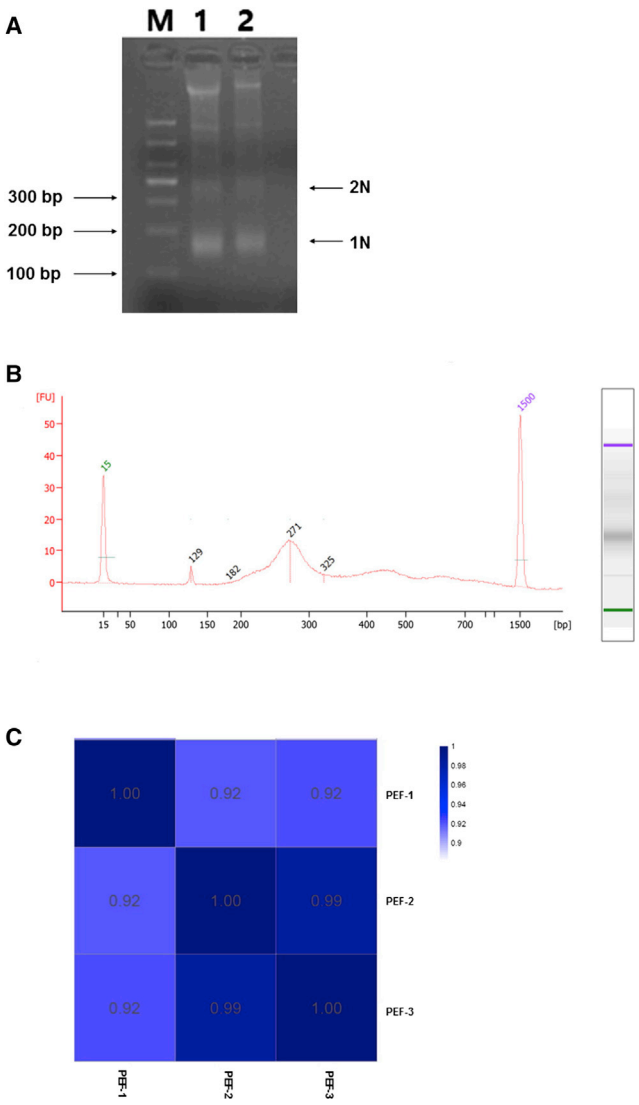

Figure 1. Establishment of MNase-Seq Using 1,000 Cells

(A) Isolation of mononucleosomes by MNase digestion of 10^6 PEF. M, 100-bp ladder; 1–2, 10^6 PEF; 1N, isolation of mononucleosomes; 2N, isolation of dinucleosomes.

(B) Detection of the adaptor-ligated mononucleosome library derived from 1,000 PEF with the Agilent 2100 Bioanalyzer.

(C) Heatmap of the Pearson correlations among PEF-1, PEF-2, and PEF-3.

1,000 fertilized zygotes, 10 hr post activation and fertilization, respectively; we then used MNase-seq to generate genome-wide maps of the nucleosome organization of porcine embryonic fibroblasts (PEF), SCNT-HMC embryos (SCNT), and fertilized zygotes (FZ). Next, we compared the nucleosome occupancies and distributions in PEF, SCNT, and FZ. Our results show that during the early stage of reprogramming, the genomes of SCNT and FZ tended toward a more open chromatin architecture compared with that of PEF. The nucleosomes around the TSSs of all genes changed from the "highly expressed" pattern in PEF to a "non-canonical" pattern in SCNT and FZ. Little transcription occurs in SCNT and FZ, which is largely determined by the nucleosome occupancy pattern around the TSS. However, the nucleosome arrangement around the TSS of some pluripotency transcription factors is the "highly expressed" pattern in SCNT and FZ. Our results provide insights into the regulation of nucleosome repositioning, as well as a basis for studying cell fate transitions during reprogramming.

RESULTS

MNase-Seq of 1,000 Cells

We derived the nucleosome maps of 1,000 SCNT-HMC reconstructed embryos 10 hr post activation, of 1,000 FZ 10 hr post fertilization, and of 1,000 PEF. First, 1×10^6 PEF were digested by MNase and subjected to gel electrophoresis (Figure 1A). The resulting mononucleosomal DNA (approximately 150 bp) was successfully isolated. We then ligated adaptors (approximately 120 bp) to the mononucleosomes for sequencing using 10^3 PEF (PEF-1), and constructed libraries as described in Experimental Procedures. The Agilent 2100 detection of the sequencing libraries is shown in Figure 1B. The peak values of the library were approximately 280 bp, corresponding to a 160-bp mononucleosome and 120-bp adaptors. These results indicated that the adaptors had been successfully ligated to the mononucleosomes, confirming the successful construction of the sequencing library. To validate the accuracy and reliability of this MNase-seq method using 1,000 cells, we carried out two additional MNase-seq experiments using 1×10^6 PEF. The Pearson correlation coefficients between the samples are shown in Figure 1C. PEF-2 is the sequencing library derived by the method described above but using 1×10^6 PEF; PEF-3 is the sequencing library derived by the sequencing company using the conventional MNase-seq method. The Pearson correlations between the samples were all greater than 0.9, indicating that all three PEF samples were highly correlated. The SDs of the fragments per kilobase per million mapped reads (FPKM) in both 500-bp and 10-kb windows of the three PEF samples (PEF-1, PEF-2 and PEF-3) were calculated and are shown in a box plot in Figure S1.

Next, we constructed the sequencing libraries of 1,000 SCNT-HMC reconstructed embryos and 1,000 FZ, which were all used 10 hr after generation. The detection of the sequencing libraries is shown in Figures 2A and 2B. These results indicated the successful construction of sequencing libraries from SCNT and FZ.

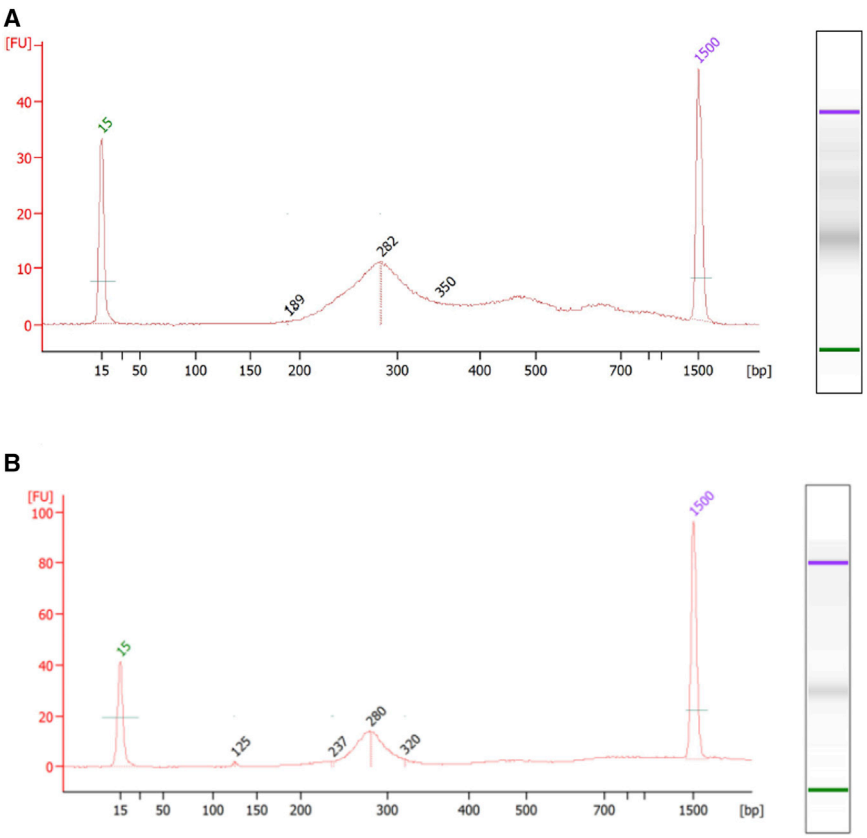

Figure 2. Agilent 2100 Detection of the Adaptor-Ligated Mononucleosome Library

(A) Sequencing library of 1,000 SCNT.

(B) Sequencing library of 1,000 FZ.

Global Nucleosome Organization and Occupancy of SCNT and PEF

To characterize their nucleosome organization and occupancy, we collected PEF, SCNT, and FZ 10 hr after generation and digested them by MNase; we then subjected the sequencing libraries to high-throughput sequencing (see Experimental Procedures). The sequencing data from this paper were deposited in the NCBI Sequence Read Archive (SRA) database under accession number SRP090055. A total of 148 million, 169 million, 165 million, 197 million, and 199 million clean reads were obtained for PEF-1, PEF-2, PEF-3, SCNT, and FZ, respectively. The details of the sequencing data and mapping information are shown in Table S1. The sequencing data showed that the MNase-seq system is effective; the detected nucleosome coverage rates for the three PEF samples were 76.08%, 74.01%, and 76.34%, while those for SCNT and FZ samples were 75.71% and 75.03% (Table S1), which indicates that the majority of the genomic DNA forms nucleosome structures.

To further elucidate the dynamics of nucleosome deposition during reprogramming, we grouped the entire porcine genome into intergenic and genic regions; each genic region was further divided into promoters, 5′ UTR, exons, introns, and 3′ UTR. Detailed information on the nucleosome occupancy in each region of the PEF, SCNT, and FZ genomes and the SD of the nucleosome occupancy in different genomic functional elements for the three PEF samples are shown in Figure 3A and Table S2. Our results showed that the nucleosome occupancies in the genic regions were 32.38%, 31.97%, and 31.62% for PEF, SCNT, and FZ, respectively, which is higher than the proportion of the genome categorized as genic regions (26.56%). However, the nucleosome occupancies in the intergenic regions (67.62%, 68.03%, and 68.38% for PEF, SCNT, and FZ, respectively) were lower than the proportion of the genome categorized as such (73.44%), which is consistent with the results of previous studies (Richmond and Davey, 2003). The nucleosome occupancy in promoters (1.53%, 1.37%, and 1.30% for PEF, SCNT, and FZ), 5′ UTR (0.19%, 0.14%, and 0.14% for PEF, SCNT, and FZ), exons (3.33%, 2.75%, and 2.54% for PEF, SCNT, and FZ), introns (26.64%, 27.03%, and 27.01% for PEF, SCNT, and FZ), and 3′ UTR (0.69%, 0.68%, and 0.62% for PEF, SCNT, and FZ) were also measured. Comparison of the ratios in each region of the PEF and SCNT genomes revealed several characteristics of nucleosome occupancy and positioning during somatic cell reprogramming. Nucleosome occupancies decreased from PEF to SCNT in all genic regions except introns; occupancy was lower in promoters (from 1.53% in

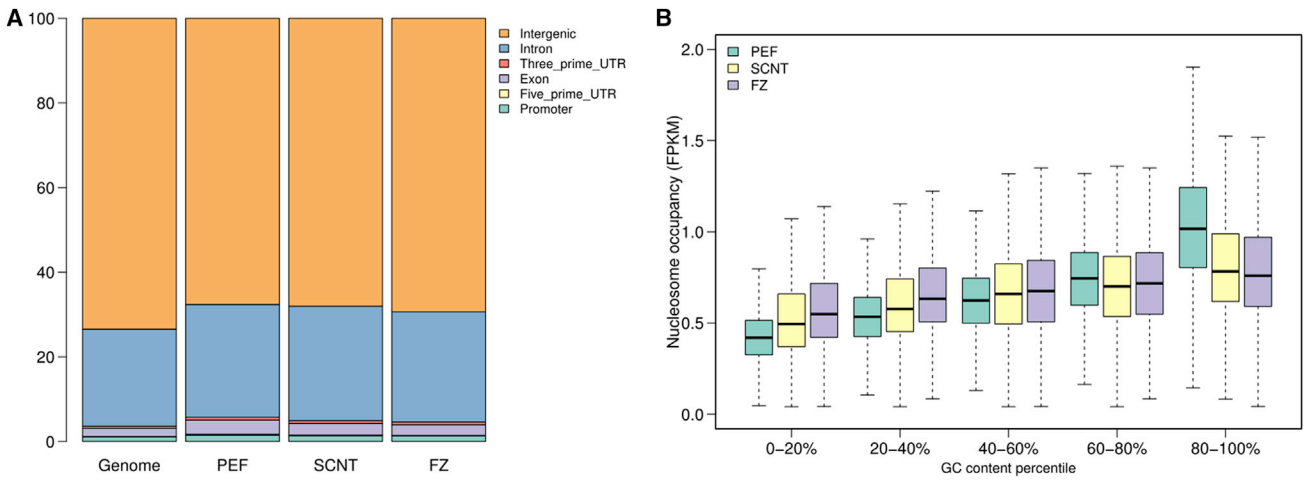

Figure 3. The Global Nucleosome Occupancy of PEF and SCNT

(A) Ratios of different functional elements in the whole genome (PEF, SCNT, and FZ). The genome bar indicates the percentage of each functional element in the porcine genome, while the PEF, SCNT, and FZ bars indicate the nucleosome occupancy for each functional element in the three samples. See also Table S2.

(B) Box plot showing the relationship between nucleosome occupancy and GC content. The blue box indicates PEF, the yellow box indicates SCNT, and the purple box indicates FZ.

PEF to 1.37% in SCNT), 5′ UTR (from 0.19% in PEF to 0.14% in SCNT), exons (from 3.33% in PEF to 2.75% in SCNT), and 3′ UTR (from 0.69% in PEF to 0.68% in SCNT). These changes in nucleosome occupancy in the promoter and genic regions may be in preparation for the next large-scale transcription events that occur during and after reprogramming. Interestingly, we found that the nucleosome occupancy of each of the functional elements of SCNT and FZ was nearly identical, indicating that the chromosome status of SCNT and FZ at the same developmental stage is similar, and that the level of reprogramming is equivalent.

We next explored the relationship between nucleosome occupancy and guanine-cytosine (GC) content. A 500-bp window was used to scan the genome, and the 500-bp fragments were divided into five bins of equal size according to their GC content. We observed a positive correlation between nucleosome occupancy and GC content in the three samples (Figure 3B). Interestingly, we found that nucleosome occupancy in PEF was lower than in SCNT in regions of low GC content (e.g., 0.41 in PEF and 0.49 in SCNT for the 0%–20% GC content bin); an increase in GC content, however, resulted in higher nucleosome occupancy in PEF than in SCNT (e.g., 1.02 in PEF and 0.78 in SCNT for the 80%–100% GC content bin). The nucleosome occupancy in regions of low GC content was higher in FZ than in the other two samples (e.g., 0.55 in FZ, 0.41 in PEF, and 0.49 in SCNT for the 0%–20% GC content bin), while in regions of high GC content, the nucleosome occupancy in FZ was similar to that in SCNT (e.g., 0.76 in FZ and 0.78 in SCNT for the 80%–100% GC content bin).

Nucleosome Occupancy Is Reorganized during Reprogramming

To characterize the dynamic chromosomal state at an early stage of reprogramming, we further compared the genome-wide nucleosome occupancy of the samples in a pairwise fashion (Figures 4A–4C). A 10-kb window was used to scan the genome. The result, shown in Figure 4A, demonstrates the changes in nucleosome occupancy across all SCNT and PEF chromosomes. We found that the nucleosome occupancy of all the SCNT chromosomes was lower than that of PEF chromosomes, especially that of the X chromosome. These findings suggest that during the early stages of somatic cell reprogramming the genome underwent substantial changes, tending toward lower nucleosome occupancy and more open chromatin architecture, which agrees with the findings of previous studies on reprogrammed induced pluripotent stem cells (iPSCs) (Huang et al., 2015). Figure 4B shows a comparison of nucleosome occupancy between the FZ and PEF chromosomes, which reveals the same trend as a comparison between the SCNT and PEF chromosomes. As expected, nucleosome occupancy was similar in SCNT and FZ (Figure 4C). Thus, the state of chromosomes changed markedly during the first few hours of reprogramming, and the reprogramming in SCNT embryos and FZ resulted in similar changes compared with PEF at the same developmental stage.

Since the X chromosome changed the most during reprogramming, we isolated all of the genes on the X chromosome and calculated the nucleosome occupancies around the TSSs in the three samples (Figures 4D–4F).

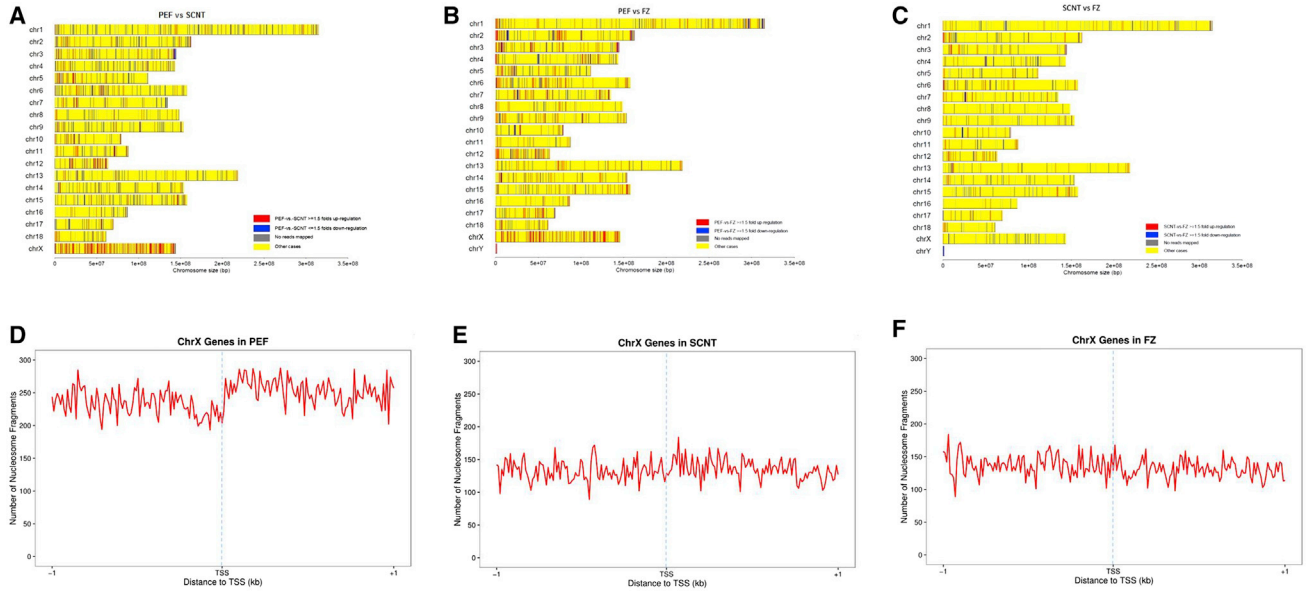

Figure 4. Dynamic Nucleosome Reorganization during Reprogramming

(A) Genome-wide comparison of the nucleosome occupancy of SCNT and PEF.

(B) Genome-wide comparison of the nucleosome occupancy of FZ and PEF.

(C) Genome-wide comparison of the nucleosome occupancy of SCNT and FZ. Colors indicate the changes in nucleosome occupancy between the samples in each 10-kb region. Red indicates that the nucleosome occupancy of sample 1 was more than 1.5-fold lower than that of sample 2, blue indicates that the nucleosome occupancy of sample 1 was more than 1.5-fold higher than that of sample 2, gray indicates the region with no reads mapped, and yellow indicates other regions.

(D) Nucleosome organization around the TSSs of all X chromosome genes in PEF.

(E) Nucleosome organization around the TSSs of all X chromosome genes in SCNT.

(F) Nucleosome organization around the TSSs of all X chromosome genes in FZ.

The nucleosome occupancies around the TSSs in SCNT and FZ were substantially lower than in PEF, while small NDRs at the TSSs were detected in PEF but not in SCNT and FZ, suggesting transcriptional activity of the genes on the X chromosome in PEF but not in SCNT and FZ.

To concretely establish the differences between the PEF and SCNT, we used a 500-bp window to scan the genome and retained the windows with a greater than 1.5-fold difference in FPKM (for details see Experimental Procedures). A total of 18,336 windows were found; among them, 11,962 windows showed that nucleosome occupancy was more than 1.5-fold lower in SCNT compared with PEF, while 6,374 windows in SCNT showed higher nucleosome occupancy (Figure 5A). This result confirmed a reduction in nucleosome occupancy and a more open chromatin state at the early stage of reprogramming.

Next, we explored the distribution of these differentially occupied windows in some important regions such as genic regions and TSSs (for details see Experimental Procedures). We found markedly greater nucleosome depletion in the regions 1 kb upstream and 10% downstream of TSS in SCNT compared with PEF (Figure 5B). We calculated the numbers of differentially occupied regions within 1 kb of TSSs, and found more windows with decreased, as opposed to increased, nucleosome occupancy in SCNT compared with PEF (Figure 5C). These results implied that nucleosome occupancy around TSSs in SCNT was lower than in PEF, especially in the region just downstream of the TSS; this suggests that the occupancy and distribution of nucleosomes (+1, +2, etc.) play important roles in gene expression and somatic cell reprogramming.

Nucleosome Arrangements around TSSs Are Linked to Gene Activity

Since the canonical nucleosome arrangement (−1, NDR, +1, +2, etc.) around TSSs is critical for gene expression (Yuan et al., 2005; Jiang and Pugh, 2009), we investigated the nucleosome organization around the TSSs of all genes in PEF, SCNT, and FZ. As expected, there was a canonical nucleosome arrangement of −1, NDR, +1, +2, etc., around the TSSs in PEF (Figures 6A and S2). However, the nucleosome organizations in SCNT and FZ were not canonical, with a slight NDR but without prominent +1 and +2 nucleosomes (Figures 6B and 6C).

To investigate the nucleosome organizations in genes that are highly expressed in PEF, and to determine how they

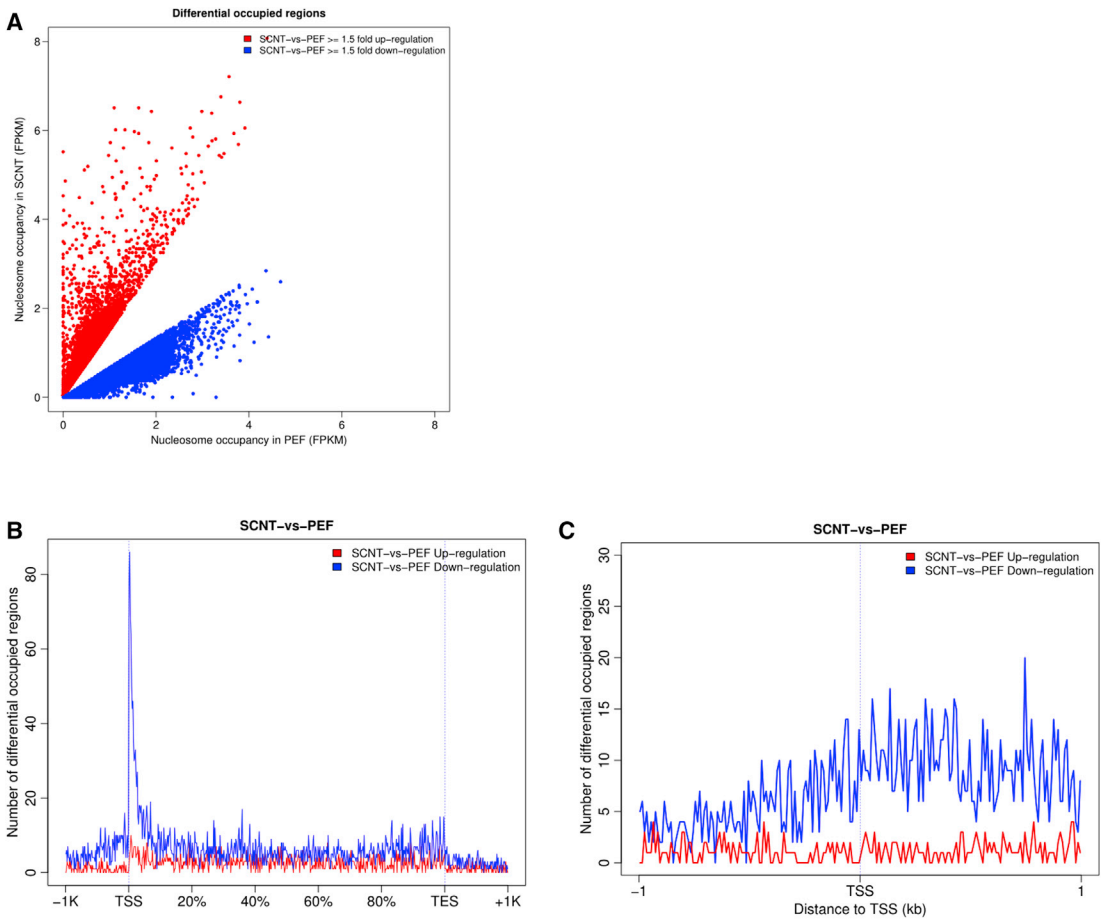

Figure 5. Differential Analysis of Nucleosome Occupancy in SCNT and PEF

(A) Differential analysis of nucleosome occupancy in PEF and SCNT. Each dot represents a window in which the nucleosome occupancy difference between the samples is more than 1.5-fold. Colors indicate the change in nucleosome occupancy in each 500-bp window between the samples. Red indicates an increase in nucleosome occupancy greater than 1.5-fold in SCNT, and blue indicates a decrease in nucleosome occupancy greater than 1.5-fold in SCNT, compared with PEF.

(B) Nucleosome distribution in genic region windows of differential nucleosome occupancy between PEF and SCNT.

(C) Nucleosome distribution around TSS windows of differential nucleosome occupancy between PEF and SCNT.

change in SCNT and FZ, we first downloaded the PEF RNA sequencing (RNA-seq) data from the NCBI (accession number GEO: GSM595679). The 22,861 genes were divided into three groups: the most highly expressed 5% of genes, silent genes, and other genes (for details see Experimental Procedures). As expected, in PEF a canonical nucleosome organization of NDR, as well as +1 and +2 nucleosomes, was found around the TSS in the most highly expressed 5% of genes and the other genes, but not in silent genes (Figures 6D and S2). Next, we examined the nucleosome organization of the same three types of genes in SCNT to explore how the nucleosome positioning of these genes changed in the early stages of somatic cell reprogramming (Figure 6E). Silent genes were barely altered, while active genes tended toward a less canonical nucleosome organization around TSSs. Nucleosome depletion at TSSs decreased in highly active and active genes, and nucleosome occupancies at +1 and +2 nucleosomes also decreased substantially in SCNT compared with PEF. These results indicated that silent genes remained silent while the transcriptional activity of the highly expressed and expressed genes in somatic cells decreased, and the genes tended to be silent at the early stage of somatic cell reprogramming. The same results were also found when comparing FZ with PEF (Figure 6F).

Nucleosome Arrangements around the TSSs of Pluripotency Genes and Fibroblast-Specific Genes

We next selected 20 common pluripotency genes or regulators (e.g., *SOX2, C-MYC,* and *DPPA2*), 18 fibroblast-specific genes (e.g., *APCDD1, IGFBP5,* and *MSX1*), and 15 common housekeeping genes (e.g., *GAPDH, TUBB,* and *ACTB*) (Tao et al., 2014; Ghosh et al., 2010; Table S3), and profiled

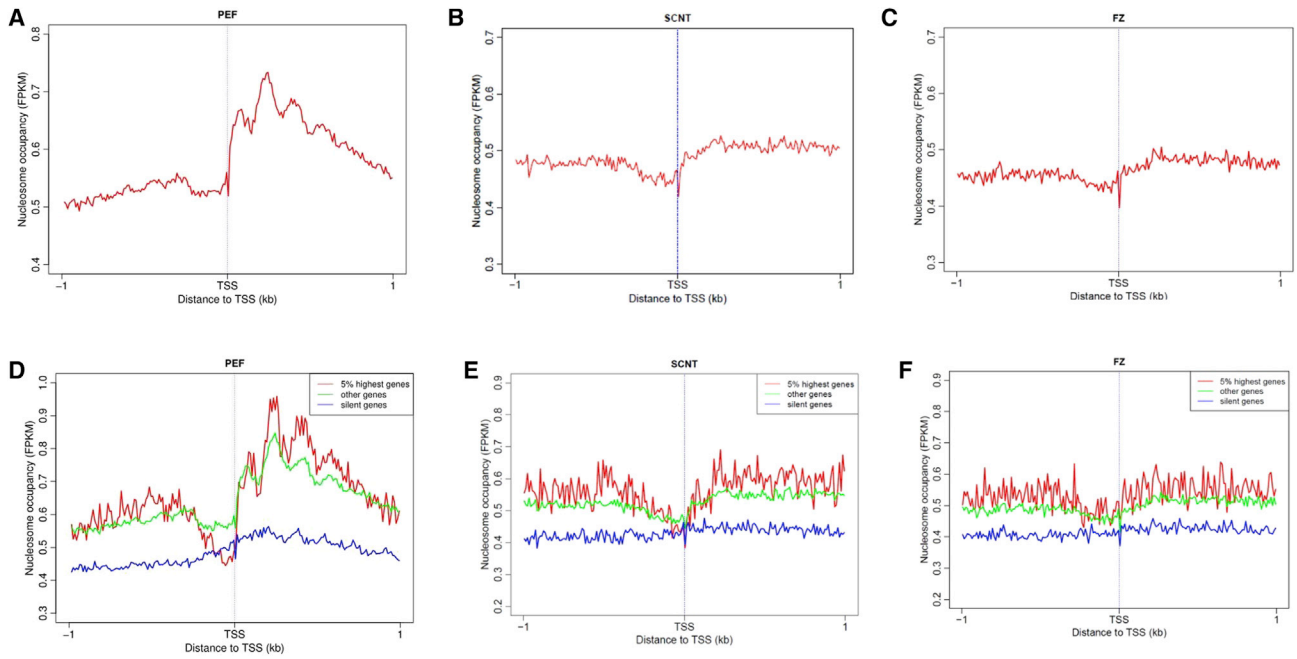

Figure 6. Nucleosome Organization around TSSs in PEF, SCNT, and FZ

(A) Nucleosome organization around the TSSs of all genes in PEF.

(B) Nucleosome organization around the TSSs of all genes in SCNT.

(C) Nucleosome organization around the TSSs of all genes in FZ.

(D–F) Nucleosome occupancy patterns around the TSSs of the most highly expressed 5% of genes (red), silent genes (blue), and other genes (green) in PEF (D), SCNT (E), and FZ (F).

See also Figure S2.

the nucleosome distribution near the TSSs of these genes (Figures 7 and S3).

The nucleosome arrangements around the TSSs of the selected pluripotency genes were typical of silent genes in PEF, but became typical of active genes in SCNT and FZ (Figures 7A, 7D, and 7G). This result suggests that pluripotency genes may be expressed or prepared for high expression in the early stages of reprogramming, indicating that they may have important functions during reprogramming. There were obvious NDRs at TSSs of fibroblast-specific genes in PEF (an active nucleosome arrangement), but the nucleosome arrangement changed to a transcriptionally silent arrangement in SCNT and FZ. In contrast, the nucleosome arrangements around the TSSs of the housekeeping genes in PEF, SCNT, and FZ were all transcriptionally active arrangements, possibly because housekeeping genes have a continuous and stable level of expression in all cell types.

DISCUSSION

Oocyte reprogramming includes a series of changes, which occur in an ordered manner and on a defined time scale (Jullien et al., 2011). The first identified events following transplantation are rapid exchanges of the mobile components of chromatin, such as linker histones and heterochromatin protein 1 (hp1), which happen within 6 hr of activation. The next step is the incorporation of the histone variant H3.3. After 24 hr, large-scale gene activation and histone H3 Lys4 dimethylation of promoters occur. Chromatin decondensation and additional histone tail modifications, such as phosphorylation, take place throughout the entire reprogramming period. Nucleosome remodeling is a dynamic process that occurs during reprogramming. Most studies focus on the chromosome status before and after reprogramming (Huang et al., 2015; Tao et al., 2014). However, the aim of this study was to explore the dynamic nucleosome positioning during the early stages of reprogramming. Thus, we selected the 10-hr post-activation time point in this study, at which complex chromatin decondensation occurs, largely in the absence of transcriptional activity. However, as documented in previous studies, it is difficult to define the difference between cells that are fully totipotent and not totipotent (Tao et al., 2014). The same problem persists in our study, as SCNT 10 hr after activation and FZ 10 hr after fertilization may

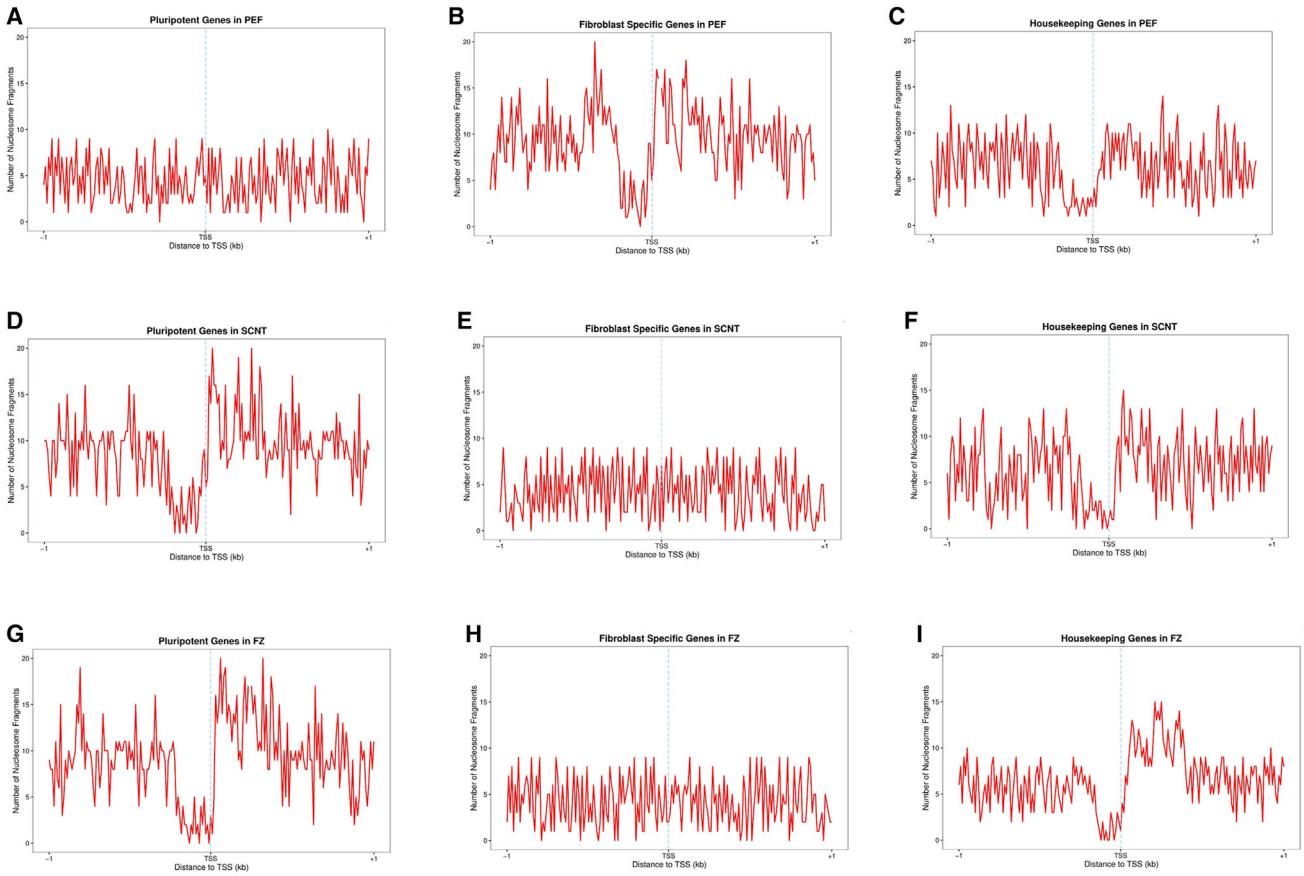

Figure 7. Nucleosome Occupancy Patterns around the TSSs of Pluripotency, Fibroblast-Specific, and Housekeeping Genes in PEF, SCNT, and FZ

Nucleosome occupancy patterns around the TSSs of selected pluripotency genes in PEF (A), fibroblast-specific genes in PEF (B), housekeeping genes in PEF (C), pluripotency genes in SCNT (D), fibroblast-specific genes in SCNT (E), housekeeping genes in SCNT (F), pluripotency genes in FZ (G), fibroblast-specific genes in FZ (H), and housekeeping genes in FZ (I). See also Figure S3.

be a mixture of embryos that are fully totipotent and not fully totipotent; however, according to previous experimental statistics, the cleavage rate of the SCNT-HMC embryos used in our research is more than 90% (Li et al., 2009), as is the cleavage rate of FZ (Liu et al., 2016), indicating that most reconstructed embryos and zygotes can be successfully reprogrammed and divided into two cells. Thus, we believe the cleavage efficiency in our study is likely to be greater than 90%.

The reprogramming mechanisms of iPSC and SCNT embryos have not been thoroughly studied, but they are known to be different. The reprogramming process in oocytes is very short and usually occurs within hours, while the factor-induced process takes days or weeks. Even though some studies have shown that human nuclear transfer-embryonic stem cells (NT-ESCs) and iPSCs have similar profiles of gene expression and DNA methylation and the same rate of *de novo* coding mutations and loss of imprinting (Johannesson et al., 2014), most findings suggest that the DNA methylation and transcriptome profiles of NT-ESCs correspond closely to those of in-vitro-fertilized ESCs, whereas iPSCs differ and retain residual DNA methylation patterns typical of parental somatic cells. Thus, SCNT is a more effective method for establishing the totipotent state and removing somatic memory than induced reprogramming (which produces iPSCs), and is therefore ideal for cell replacement therapies (Ma et al., 2014; Chin et al., 2009; Ghosh et al., 2010; Doi et al., 2009; Lister et al., 2011). Another concern is that certain differentiation deficiencies have been reported in human iPSCs. In addition, it has been challenged that genome integrity is not maintained during the process of induced reprogramming, with reports showing that *de novo* mutations and copy-number variations might be introduced in iPSCs. Finally, iPSCs were found to harbor a residual epigenetic signature characteristic of their donor cells (Kim et al.,

2010; Polo et al., 2010). These so-called epigenetic memories restrict their fate choice following differentiation. In contrast, mouse pluripotent cells generated through SCNT did not appear to show such memories. However, in this study we found that the chromosomes in SCNT embryos and FZ both tended toward nucleosome loss and more open chromatin architecture within a few hours of reprogramming, especially in the X chromosome; similar changes occur in iPSC reprogramming (Tao et al., 2014; Huang et al., 2015).

In this study, we show that the coverage rate and nucleosome occupancy decreased in promoters in SCNT compared with PEF. Although previous studies have shown that nucleosome loss in promoters can lead to high transcriptional activity (Segal et al., 2006), SCNT have been shown to have little global transcriptional activity at the early stage of reprogramming (Jullien et al., 2011). Thus, we conclude that the transcriptional activity of genes is not only determined by the nucleosome occupancy but also by the nucleosome arrangement in the promoter. In our study, nucleosome occupancy increased in coding regions, from 29.58% in PEF to 31.97% in SCNT and 30.31% in FZ, but decreased in promoter regions, from 1.42% in PEF to 1.37% in SCNT and 1.3% in FZ. These changes may be in preparation for the upcoming large-scale transcription events. Nucleosome occupancy increased with increasing GC content. Given that there is a positive correlation between GC content and gene density, the increase in nucleosome occupancy in regions with high GC content indicates there are more nucleosomes in the genic region. In addition, nucleosome occupancy in PEF was greater than that in SCNT across regions with different GC content, suggesting a more pyknotic chromatin structure in PEF.

In somatic cells, the induction of totipotency can result in reactivation of the silent inactive X chromosome (Cantone et al., 2016). A strong correlation between totipotency and X chromosome reactivation has been shown in experimental mouse cell reprogramming studies (Ohhata and Wutz, 2013). In this study, we observed a similar result 10 hr post activation. The nucleosome occupancy changes on the X chromosome indicate that the reactivation of the X chromosome had already occurred at this time point. The substantial decrease in nucleosome occupancy in promoters around TSSs may be in preparation for the expression of X chromosome genes, which is crucial for the process of reprogramming. PEF, but not SCNT, have a canonical nucleosome arrangement around TSSs, which supports the scant transcriptional activity in SCNT, and may be due to the structures of nucleosomes around the TSSs. The nucleosome rearrangements at genes with differing expression levels in PEF also indicated that silent genes remained silent in SCNT and FZ, while canonical nucleosome structures were not detected in SCNT and FZ.

Fibroblast-specific genes are expressed only in fibroblasts; we found that the nucleosome arrangements around the TSSs of these genes were consistent with high expression in PEF, but changed to a silent arrangement after reprogramming, indicating that these genes are not expressed in SCNT and FZ. However, some pluripotency genes are required in the process of reprogramming, and changes in nucleosome occupancy and positioning at these genes during reprogramming are critical. The nucleosome occupancy of these genes indicated nucleosome depletion at the TSSs in SCNT and FZ compared with PEF, suggesting that these genes have been or will soon be expressed in the cells undergoing reprogramming. The nucleosome structures around the TSSs of housekeeping genes remained unchanged, possibly due to their continuous expression in all cell types. Our results indicate that the chromatin of the reconstructed embryos and zygotes changed substantially 10 hr after activation and fertilization, leading to scant global transcription.

EXPERIMENTAL PROCEDURES

All experiments were performed in accordance with the guide for the Care and Use of Laboratory Animals prepared by the Institutional Animal Care and Use Committee of Nanjing Agricultural University, China.

Oocyte Collection and *In Vitro* Maturation

Ovaries from 7- to 8-month-old commercial pigs were obtained from a local slaughterhouse, placed into normal saline supplemented with streptomycin and penicillin at 37°C, and transported in a thermos. Five- to 8-mm follicles were selected, and an 18-gauge needle attached to a 10-mL disposable syringe was used to aspirate the follicular fluid. The cumulus-oocyte complexes with multiple layers of intact cumulus cells and uniform ooplasm were separated by vacuum suction according to their morphological characteristics and washed twice in wash buffer. *In vitro* maturation, conducted in 4-well dishes in TCM-199 culture medium, included incubation at 38.5°C with 5% CO_2 in air, at maximum humidity, for 42–44 hr (Vajta et al., 1997).

SCNT-HMC

Oriented Handmade Enucleation

The basic manipulations of HMC have been previously described (Li et al., 2009). In brief, after 42 hr of *in vitro* maturation we removed the cumulus cells from the cumulus-oocyte complex and incubated the denuded oocytes in 3.3 mg/mL pronase dissolved in T33 (TCM-199 with 33% [v/v] cattle serum) for 20 s to remove the zona pellucida, then washed them twice with T2 (TCM-199 with 2% [v/v] cattle serum) and T20 (TCM-199 with 20% [v/v] cattle serum), and transferred them to a T2 drop with 2.5 μg/mL cytochalasin B. We used a fire-polished glass capillary to rotate the oocytes to make the extrusion of the polar body visible under the stereomicroscope. The oocytes were then bisected

with a microblade. After the bisection, the halves of the cytoplasts of oocytes without polar bodies were selected and transferred to T2 drops for further fusion.

Two-Step Fusion and Activation

Approximately 200 PEF donor cells were prepared in a T2 drop after trypsinization. All of the cytoplasts of the oocytes were incubated in T10 (TCM-199 with 10% [v/v] cattle serum) drops for a short time and transferred individually to 1 mg/mL phytohemagglutinin for 2–3 s, then dropped down over single donor cells in T2 drops to form cytoplast-PEF pairs. The pairs were then aligned to one wire of a fusion chamber (BTX) by an alternating current of 0.06 kV/cm and 700 kHz, then fused with a single direct current (DC) impulse of 2.0 kV/cm for 9 μs by an electrofusion machine (BLS). After 1-hr incubation in T10 drops, the successfully fused pairs were selected and transferred into the activation medium. The experimental manipulations for the second fusion were similar to those of the first fusion described above, except that the DC impulse was 0.86 kV/cm for 80 μs. Fusion was again observed in a T10 drop after a 15-min incubation period. We used chemical activation after the two-step fusion. The selected, successfully fused, reconstructed embryos were then transferred to porcine zygote medium-3 culture solution for further culture.

In Vitro Fertilization

Fresh semen was washed three times with Dulbecco's PBS supplemented with 0.1% BSA, 75 μg/mL penicillin G, and 50 μg/mL streptomycin, and centrifuged at 100 × *g* for 3 min. We removed the supernatant, resuspended the spermatozoa pellets in fertilization medium (modified Tris-buffered medium, containing 2 mg/mL BSA [fraction V] plus 2 mM caffeine), and diluted the suspension to 0.5×10^6 to 1.5×10^6 sperm/mL. Groups of 25 denuded oocytes were washed three times in fertilization medium, then transferred to 100 μL fertilization medium covered with paraffin oil. Fifty microliters of diluted spermatozoa (around 0.5×10^6 to 1.5×10^6 sperm/mL) was added to 100 μL of fertilization medium containing oocytes, for a final sperm concentration of 1.5×10^5 to 5.0×10^5 sperm/mL. The oocytes were incubated with the sperm for 10 hr at 38.5°C with 5% CO_2 in air.

MNase-Seq

All chemicals were purchased from New England Biolabs unless otherwise stated. PEF-1, PEF-2, PEF-3, 1,000 reconstructed embryos cultured 10 hr after activation, and 1,000 fertilized zygotes cultured 10 hr after fertilization were treated with a Nucleosomal DNA Prep Kit (D5220; Zymo Research) according to the manufacturer's instructions. Mononucleosome fragments were derived after the treatment, and the sequencing library was prepared using the NEBNext Ultra DNA Library Prep Kit (E7370; New England Biolabs) according to the manufacturer's instructions. In brief, mononucleosome fragments were blunt-ended and a dA tail was added. Illumina genomic adaptors with index sequences were ligated to DNA fragments with dA tails, and adaptor-ligated DNA was amplified by PCR using indexed primers for 12 cycles. Each step was followed by purification using AMPure XP Beads (Beckman Coulter, #A63881). The libraries were generated with a mean insertion size of 160 bp, and tested with a 2100 Bioanalyzer (Agilent Technologies). Sequencing of 100-bp paired-end reads on a HiSeq 2000 was performed by Novogene.

Global Nucleosome Occupancy Calculation

The sequence reads were aligned with the *Sus scrofa* (pig) reference genome (*Sscrofa 10.2*, http://asia.ensembl.org/Sus_scrofa/Info/Index) by Bowtie2, and all uniquely matching reads were retained. To analyze the relationship between nucleosome occupancy and GC content, we divided the 500-bp fragments into five bins according to their GC content, and their FPKM values were calculated.

Comparison of Nucleosome Occupancy in Each Chromosome

For each chromosome, nucleosome read counts were binned in 10-kb intervals and divided by the total number of uniquely mapped reads. Comparisons between samples were conducted bin-by-bin for each chromosome. Different colors were used to represent the fold change in nucleosome occupancy among the three samples; red indicates that the nucleosome occupancy of sample 1 was more than 1.5-fold lower than that of sample 2, blue indicates that the nucleosome occupancy of sample 1 was more than 1.5-fold higher than that of sample 2, gray indicates regions with no reads mapped, and yellow indicates other regions.

Nucleosome Occupancy in Different Regions of the Genome

Nucleosome distribution across the genome was further explored by calculating the percentage of nucleosome reads in discrete regions (i.e., promoters, 5′ UTR, exons, introns, 3′ UTR, and intergenic regions). The specific sequence information for these regions, corresponding to the reference genome *Sscrofa 10.2*, was downloaded from the University of California at Santa Cruz (UCSC) Genome Bioinformatics. The nucleosome occupancy in each region was calculated using BEDTools software (version 2.16.2) (Huang et al., 2015), and the nucleosome occupancy ratio in each region was determined. The results were compared with the ratios of the different regions in the genome.

Nucleosome Distribution Profiles

The gene annotation file was downloaded from UCSC. Nucleosomes within 1 kb of each TSS were collected. The total 2-kb length was binned in 10-bp intervals, and the FPKM value or the number of nucleosome fragments in each bin was calculated to obtain a profile of the nucleosome distribution around the TSS (Huang et al., 2015).

Genome-wide Comparison of Nucleosome Occupancy

Nucleosome occupancy calculations were performed using the same approach as described above, and the whole genome was scanned with a 500-bp window. The FPKM value was calculated in each window and compared pairwise between samples for the differential analysis. Windows in which the FPKM value was upregulated or downregulated 1.5-fold were retained for further analysis. The differential window numbers were calculated to explore their distribution in genic regions and around TSSs. The

calculation method was the same as that used for the nucleosome distribution profiles.

Gene Expression Analysis

The PEF RNA-seq data were downloaded from the GEO (accession number GEO: GSM595679) of the NCBI. The RNA-seq reads were mapped to the UCSC genes (version susScr3) using HISAT. All uniquely matching alignments were retained for analysis. HTSeq software was employed to calculate the reads number for each gene, which were normalized as an FPKM value. Genes were classified into three types according to their expression levels: the most highly expressed 5% of genes, silent genes, and all other genes. Nucleosome distribution profiles around TSSs were calculated in the same manner as described above.

SUPPLEMENTAL INFORMATION

Supplemental Information includes three figures and three tables and can be found with this article online at http://dx.doi.org/10.1016/j.stemcr.2017.06.004.

AUTHOR CONTRIBUTIONS

H.L. conceived and supervised the study; J. Li, B.C., D.C., Y.Z., Y.N., and C.W. performed the SCNT-HMC experiments; X.Z. and W.C. performed the fertilization experiments; and Z.P. and C.T. uploaded the sequencing data to the SRA database. C.T., W.W., J. Lian, and Y.-L.M. analyzed the data and prepared the manuscript. All authors read and approved the final manuscript.

ACKNOWLEDGMENTS

This work was supported by the 973 Program (2014CB138502), the National Natural Science Foundation of China (31472073), the State Key Program of National Natural Science Foundation of China (31630072), the National Natural Science Foundation of China (31501920), the Priority Academic Program Development of Jiangsu Higher Education Institutions (PAPD), and the National Key Research and Development Program of China, Stem Cell and Translational Research (grant no. 2016YFA0100203).

Received: October 28, 2016
Revised: June 6, 2017
Accepted: June 6, 2017
Published: July 6, 2017

REFERENCES

Bernstein, B.E., Liu, C.L., Humphrey, E.L., Perlstein, E.O., and Schreiber, S.L. (2004). Global nucleosome occupancy in yeast. Genome Biol. *5*, R62.

Cantone, I., Bagci, H., Dormann, D., Dharmalingam, G., Nesterova, T., Brockdorff, N., Rougeulle, C., Vallot, C., Heard, E., Chaligne, R., et al. (2016). Ordered chromatin changes and human X chromosome reactivation by cell fusion-mediated pluripotent reprogramming. Nat. Commun. *7*, 12354.

Chin, M.H., Mason, M.J., Xie, W., Volinia, S., Singer, M., Peterson, C., Ambartsumyan, G., Aimiuwu, O., Richter, L., Zhang, J., et al. (2009). Induced pluripotent stem cells and embryonic stem cells are distinguished by gene expression signatures. Cell Stem Cell *5*, 111–123.

Doi, A., Park, I.H., Wen, B., Murakami, P., Aryee, M.J., Irizarry, R., Herb, B., Ladd-Acosta, C., Rho, J., Loewer, S., et al. (2009). Differential methylation of tissue- and cancer-specific CpG island shores distinguishes human induced pluripotent stem cells, embryonic stem cells and fibroblasts. Nat. Genet. *41*, 1350–1353.

Du, Y., Kragh, P.M., Zhang, Y., Li, J., Schmidt, M., Bøgh, I.B., Zhang, X., Purup, S., Jørgensen, A.L., Pedersen, A.M., et al. (2007). Piglets born from handmade cloning, an innovative cloning method without micromanipulation. Theriogenology *68*, 1104–1110.

Field, Y., Kaplan, N., Fondufe-Mittendorf, Y., Moore, I.K., Sharon, E., Lubling, Y., Widom, J., and Segal, E. (2008). Distinct modes of regulation by chromatin encoded through nucleosome positioning signals. PLoS Comput. Biol. *4*, e1000216.

Ghosh, Z., Wilson, K.D., Wu, Y., Hu, S., Quertermous, T., and Wu, J.C. (2010). Persistent donor cell gene expression among human induced pluripotent stem cells contributes to differences with human embryonic stem cells. PLoS One *5*, e8975.

Huang, K., Zhang, X., Shi, J., Yao, M., Lin, J., Li, J., Liu, H., Li, H., Shi, G., Wang, Z., et al. (2015). Dynamically reorganized chromatin is the key for the reprogramming of somatic cells to pluripotent cells. Sci. Rep. *5*, 17691.

Jiang, C., and Pugh, B.F. (2009). A compiled and systematic reference map of nucleosome positions across the *Saccharomyces cerevisiae* genome. Genome Biol. *10*, R109.

Johannesson, B., Sagi, I., Gore, A., Paull, D., Yamada, M., Golan-Lev, T., Li, Z., LeDuc, C., Shen, Y., Stern, S., et al. (2014). Comparable frequencies of coding mutations and loss of imprinting in human pluripotent cells derived by nuclear transfer and defined factors. Cell Stem Cell *15*, 634–642.

Jullien, J., Pasque, V., Halley-Stott, R.P., Miyamoto, K., and Gurdon, J.B. (2011). Mechanisms of nuclear reprogramming by eggs and oocytes: a deterministic process. Nat. Rev. Mol. Cell Biol. *12*, 453–459.

Kaplan, N., Moore, I.K., Fondufe-Mittendorf, Y., Gossett, A.J., Tillo, D., Field, Y., LeProust, E.M., Hughes, T.R., Lieb, J.D., Widom, J., et al. (2009). The DNA-encoded nucleosome organization of a eukaryotic genome. Nature *458*, 362–366.

Kim, K., Doi, A., Wen, B., Ng, K., Zhao, R., Cahan, P., Kim, J., Aryee, M.J., Ji, H., Ehrlich, L.I., et al. (2010). Epigenetic memory in induced pluripotent stem cells. Nature *467*, 285–290.

Kragh, P.M., Nielsen, A.L., Li, J., Du, Y., Lin, L., Schmidt, M., Bøgh, I.B., Holm, I.E., Jakobsen, J.E., Johansen, M.G., et al. (2009). Hemizygous minipigs produced by random gene insertion and handmade cloning express the Alzheimer's disease-causing dominant mutation APPsw. Transgenic Res. *18*, 545–558.

Kurome, M., Ishikawa, T., Tomii, R., Ueno, S., Shimada, A., Yazawa, H., and Nagashima, H. (2008). Production of transgenic and non-transgenic clones in miniature pigs by somatic cell nuclear transfer. J. Reprod. Dev. *54*, 156–163.

Lee, C.K., Shibata, Y., Rao, B., Strahl, B.D., and Lieb, J.D. (2004). Evidence for nucleosome depletion at active regulatory regions genome-wide. Nat. Genet. *36*, 900–905.

Lee, W., Tillo, D., Bray, N., Morse, R.H., Davis, R.W., Hughes, T.R., and Nislow, C. (2007). A high-resolution atlas of nucleosome occupancy in yeast. Nat. Genet. *39*, 1235–1244.

Li, J., Du, Y., Zhang, Y.H., Kragh, P.M., Purup, S., Bolund, L., Yang, H., Xue, Q.Z., and Vajta, G. (2006). Chemically assisted handmade enucleation of porcine oocytes. Cloning Stem Cells *8*, 241–250.

Li, J., Villemoes, K., Zhang, Y., Du, Y., Kragh, P.M., Purup, S., Xue, Q., Pedersen, A.M., Jørgensen, A.L., Jakobsen, J.E., et al. (2009). Efficiency of two enucleation methods connected to handmade cloning to produce transgenic porcine embryos. Reprod. Domest. Anim. *44*, 122–127.

Li, J., Li, R., Villemoes, K., Liu, Y., Purup, S., and Callesen, H. (2015). Developmental potential and kinetics of pig embryos with different cytoplasmic volume. Zygote *23*, 277–287.

Lister, R., Pelizzola, M., Kida, Y.S., Hawkins, R.D., Nery, J.R., Hon, G., Antosiewicz-Bourget, J., O'Malley, R., Castanon, R., Klugman, S., et al. (2011). Hotspots of aberrant epigenomic reprogramming in human induced pluripotent stem cells. Nature *471*, 68–73.

Liu, Y., Wang, H., Lu, J., Miao, Y., Cao, X., Zhang, L., Wu, X., Wu, F., Ding, B., Wang, R., et al. (2016). Rex rabbit somatic cell nuclear transfer with in vitro-matured oocytes. Cell. Reprogram. *18*, 187–194.

Luger, K., Mäder, A.W., Richmond, R.K., Sargent, D.F., and Richmond, T.J. (1997). Crystal structure of the nucleosome core particle at 2.8 A resolution. Nature *389*, 251–260.

Ma, H., Morey, R., O'Neil, R.C., He, Y., Daughtry, B., Schultz, M.D., Hariharan, M., Nery, J.R., Castanon, R., Sabatini, K., et al. (2014). Abnormalities in human pluripotent cells due to reprogramming mechanisms. Nature *511*, 177–183.

Ohhata, T., and Wutz, A. (2013). Reactivation of the inactive X chromosome in development and reprogramming. Cell. Mol. Life Sci. *70*, 2443–2461.

Polo, J.M., Liu, S., Figueroa, M.E., Kulalert, W., Eminli, S., Tan, K.Y., Apostolou, E., Stadtfeld, M., Li, Y., Shioda, T., et al. (2010). Cell type of origin influences the molecular and functional properties of mouse induced pluripotent stem cells. Nat. Biotechnol. *28*, 848–855.

Richmond, T.J., and Davey, C.A. (2003). The structure of DNA in the nucleosome core. Nature *423*, 145–150.

Segal, E., Fondufe-Mittendorf, Y., Chen, L., Thåström, A., Field, Y., Moore, I.K., Wang, J.P., and Widom, J. (2006). A genomic code for nucleosome positioning. Nature *442*, 772–778.

Tao, Y., Zheng, W., Jiang, Y., Ding, G., Hou, X., Tang, Y., Li, Y., Gao, S., Chang, G., Zhang, X., et al. (2014). Nucleosome organizations in induced pluripotent stem cells reprogrammed from somatic cells belonging to three different germ layers. BMC Biol. *12*, 109.

Vajta, G., Holm, P., Greve, T., and Callesen, H. (1997). The Submarine Incubation System, a new tool for in vitro embryo culture. A technique report. Theriogenology *48*, 1379–1385.

Vajta, G., Lewis, I.M., Trounson, A.O., Purup, S., Maddox-Hyttel, P., Schmidt, M., Pedersen, H.G., Greve, T., and Callesen, H. (2003). Handmade somatic cell cloning in cattle: analysis of factors contributing to high efficiency in vitro. Biol. Reprod. *68*, 571–578.

Yoshioka, K., Suzuki, C., Tanaka, A., Anas, I.M., and Iwamura, S. (2002). Birth of piglets derived from porcine zygotes cultured in a chemically defined medium. Biol. Reprod. *66*, 112–119.

Yuan, G.C., Liu, Y.J., Dion, M.F., Slack, M.D., Wu, L.F., Altschuler, S.J., and Rando, O.J. (2005). Genome-scale identification of nucleosome positions in S. cerevisiae. Science *309*, 626–630.